DUPLICATE ALSO

METEOROLOGICAL OFFICE

Forecasting Research

Forecasting Research Division
Scientific Paper No. 25

The 1D, Vertical, Version of the Proposed Semi-Implicit Integration Scheme for the Unified Model: Formulation and Test Results

by

S. Coulter, M.H. Mawson and M.J.P. Cullen

November 1994

Meteorological Office
London Road
Bracknell
Berkshire
RG12 2SZ
United Kingdom

ORGS UKMO F

National Meteorological Library
FitzRoy Road, Exeter, Devon. EX1 3PB

Forecasting Research Scientific Paper No. 25

The 1D, Vertical, Version of the Proposed Semi-Implicit Integration Scheme for the Unified Model: Formulation and Test Results.

S. Coulter, M. H. Mawson and M. J. P. Cullen

November 1994

This document has not been published. Permission to quote from it must be obtained from the director of Forecasting Research.

© Crown Copyright 1994.

Abstract

This paper describes the 1D, vertical, version of the proposed semi-implicit integration scheme for the Unified Model, see Cullen et al [1] for details of the full 3D proposal. The dry formulation of the equations is presented along with the 1D version of the numerical algorithm. To investigate the numerical stability of the algorithm two test problems are used. The first uses a density perturbation to force the model and can be considered as being similar to an 'organ pipe'. The second test problem is that of explicit convection in a neutrally stable column. Results for both problems are presented and it is seen that the proposed scheme performs very well.

1 1D equations and algorithm.

The full proposal for the semi-implicit integration scheme for the Unified Model can be found in Cullen et al [1]. Here we summarise the main points;

- Non-hydrostatic Primitive equations
- semi-implicit, semi-Lagrangian integration scheme
- uses the distance from the centre of the earth as the vertical co-ordinate
- uses a Charney-Phillips vertical grid staggering
- uses a C-grid horizontal staggering

In this paper we consider the 1D, vertical, version of the model in the absence of moisture and physics and in this form we do not see the effects of the horizontal grid staggering. In the proposed model there are two vertical co-ordinates; the distance from the centre of the earth, denoted r, which can vary with horizontal position on a model level and a generalised vertical co-ordinate η which does not vary with horizontal position on a model level and satisfies $\eta = 0$ at the earth's surface and $\eta = 1$ at the upper boundary. In this 1D model there exists a trivial linear relationship between r and η at any level k given by

$$\eta(k) = \frac{r(k) - r(0)}{r(N) - r(0)}$$

where level 0 is the earth's surface and level N the value at the upper boundary. This relationship in the 3D model can be general and no simple formula may exist. The semi-Lagrangian scheme is a two-time-level scheme described for the full 3D model in Mawson [3]. The Charney-Phillips vertical grid staggering is shown in figure 1 where the levels indicated correspond to the indexing in the computer code noting that level $k = .5$ is referred to in the code as level 1. For simplicity we refer to model levels as *theta levels* if we wish to refer to a quantity at a level where θ is held, and to *rho levels* if we wish to refer to a quantity at a level where ρ is held.

Upper Boundary	r,η,θ,w,$\dot{\eta}$	k=N
	r,η,ρ,p	k=N-0.5
	.	
	.	
	.	
	r,η,θ,w,$\dot{\eta}$	k=1.0
	r,η,ρ,p	k=0.5
	r,η,θ,w,$\dot{\eta}$	k=1.0
	r,η,ρ,p	k=0.5
surface	r,η,w,$\dot{\eta}$	k=0

Figure 1: Charney-Phillips grid staggering

1.1 1D dry equations

The 1D dry versions of the equations given in Cullen et al[1] are

$$\frac{Dw}{Dt} + g + C_p\theta\frac{\partial \Pi}{\partial r} = 0 \tag{1.1}$$

$$\frac{D\theta}{Dt} = 0 \tag{1.2}$$

$$\frac{\partial \rho}{\partial t} + \frac{1}{\partial r/\partial \eta}\left[\frac{\partial}{\partial \eta}\left(\rho\dot{\eta}\frac{\partial r}{\partial \eta}\right)\right] = 0 \tag{1.3}$$

$$\Pi^{\frac{\kappa-1}{\kappa}}\theta\rho = \frac{p_{ref}r^2}{\kappa C_p} \tag{1.4}$$

where $\Pi = (p/p_{ref})^\kappa$ is the Exner pressure with p_{ref} a reference pressure value, and

$$\frac{dr}{d\eta}\dot{\eta} = w \tag{1.5}$$

As in Cullen et al [1] the density, ρ, includes a factor of r^2 and hence is related to the true density, ρ_t via $\rho = r^2\rho_t$. The boundary conditions imposed are that $w = 0$ at the surface and upper boundary, and using equation (1.5) we obtain $\dot{\eta} = 0$ at the surface and upper boundary also.

1.2 Numerical Algorithm

The numerical algorithm described in this section is known as a predictor/corrector method. The basic idea of such algorithms is as follows: use the prognostic equations to predict the values of the variables at the new time level. Then insist that these predicted variables satisfy some equation(s) at the new time level. For example, in the algorithm we will describe here we require that the variables satisfy the equation of state at the new time level. In general they will not satisfy these equation(s) and we form a correction equation to find the corrections to these variables to make these equation(s) hold. Having solved the correction equation the resulting corrections are added onto the predicted variables to obtain the final values at the new time level. To understand this approach it may help to think of the solution evolving along some path in solution space. Then to find the solution at some future time we need to know the path the solution follows. The predictor/corrector approach seeks to find this path by producing an estimate of it, given by the predictor step, and then use some measure of the error, the equations to be satisfied at the new time, to correct this estimate.

In many cases the correction equation is highly complex and very difficult to solve. To alleviate this problem it is often possible to simplify the correction equation and use an iterative technique to find the solution to the full correction equation. This approach will be adopted here, but no iterations will be perfomed. This is because it is expected that the solution obtained from the simplified equation will be close enough to the solution of the full equation so that no benefit will accrue from iterating the procedure.

The main purpose of the 1D tests presented here is to investigate the computational stability of the proposed algorithm. The scheme can be made more or less stable by changed the time-weighting parameters, denoted by α_i. These parameters control the time-averaging of various terms in the scheme with the time-average of a quantity c being given by

$$\overline{c}^{ti} = (1 - \alpha_i)c^n + \alpha_i c^{n+1}$$

Linear stability arguments imply that all the α_i's satisfy

$$0.5 \leq \alpha_i \leq 1$$

To obtain second order accuracy in time all the α_i's must be set to 0.5, but this is also the limiting value for stability. In practice most algorithms cannot be run with values on the stability limit and remain stable, usually because of rounding error or non-linear instability, and a value greater than the lower bound is required. Golding [2] found that for the 1D version of the old non-hydrostatic Meteorological Office Mesoscale model a value of 0.7 was required to suppress computational noise for the first test problem we attempt here. In the full 3D model there are 7 different α's refered to as α_1 to α_6 and α_w. In the 1D scheme α_1, α_3 and α_6 do not appear. In the algorithm that follows we use the notation subscript d to denote a value at the departure point of a trajectory, superscripts n and $n+1$ to denote the current and future time-levels, with Δt the timestep, and the usual finite-difference notation for a quantity c

$$\delta_r c = (c(r + \frac{\Delta r}{2}) - c(r - \frac{\Delta r}{2}))/\Delta r$$

$$\overline{c}^r = (c(r + \frac{\Delta r}{2}) + c(r - \frac{\Delta r}{2}))/2$$

with similar definitions for $\delta_\eta c$ and $\overline{c}^\eta$.

We also adopt the notation of Cullen et al [1] with the exception that p_0 in their notation is referred to as p_{ref} and we use subscript 0 to denote a value at the surface instead of subscript $*$. The semi-Lagrangian choices listed in the algorithm are the ones we used, and are the same as those given in Cullen et al [1]. More accurate choices can be made, for example higher order interpolation can be used, see Mawson [3] for currently available alternatives.

Step 1. Calculate $\dot{\eta}$

$$\dot{\eta} = \frac{w}{\delta_\eta r} \tag{1.6}$$

Step 2. Calculate an estimate of the advection increments to θ. The semi-Lagrangian scheme uses w^n to find the departure point and linear interpolation

to obtain θ at the departure point. Conservation was not enforced in this step.

$$S_4 = \theta_d^n - \theta^n \tag{1.7}$$

Step 3. Include any potential temperature forcing, denoted by Q.

$$\theta^* = \theta^n + S_4 + Q \tag{1.8}$$

$$R_4 = \theta^* - \theta^n \tag{1.9}$$

Note:

For the first test problem we consider in section 2 $Q = 0$. For the second test problem Q is equal to the temperature perturbation multiplied by the timestep.

Step 4. Calculate the residual, R_3, for the time discretized form of the vertical momentum equation (1.1). The semi-Lagrangian scheme uses w^n to find the departure point and linear interpolation to obtain the terms at the departure point. Conservation was not enforced in this step.

$$R_3 = w_d^n - w^n + \Delta t\left((1-\alpha_w)[g - C_p\theta^n\delta_r\Pi^n]_d + \alpha_w[g - C_p\theta^n\delta_r\Pi^n]\right) \tag{1.10}$$

Notes:

i. This step is not repeated after the Helmholtz equation is solved, and hence a better estimate of these terms is not obtained, whereas step 2 which calculates the corresponding residual for the potential temperature is repeated. In the full 3D algorithm the only step not repeated is the one for the vertical velocity and the reason given is that the terms are small compared to other terms. In the full 3D model this maybe true but in this 1D model this is debatable. It is likely that a better solution could be obtained by repeating this step as is done for potential temperature. Also the forcing term in this equation is only formally first order accurate in time but if the step is repeated, in principle, it can be made second order accurate if $\alpha_w = 0.5$. For energetic consistency we should perform the second advection step since the kinetic energy evolution equation is in terms of w_1. However the forcing function should not be evaluated at time level $n+1$ since it is assumed to be at time level n.

This restriction might be removable but would require the proof of energetic consistency to be re-examined. See Appendix B for the details of the energetic consistency proofs.

ii. The formulation of the pressure gradient term in the equations used to calculate R_3 implies a particular vertical averaging of ρ

$$\tilde{\rho}^r = \frac{r^2 \delta_r p}{C_p \theta \delta_r \Pi} \tag{1.11}$$

This definition of ρ is used to find ρ on θ levels and via the equation of state (1.4) to define p and Π on θ levels, with the exception of the top θ level. The pressure at the top is derived by assuming the hydrostatic equation above the top ρ level to give

$$p_N = p - \frac{\rho g}{r^2}(r_N - r)$$

where all the quantities are evaluated at the top ρ level except those with subscript N which are evaluated at the top θ level. A similar assumption of the hydrostatic equation below the bottom ρ level allows calculation of the surface pressure

$$p_0 = p + \frac{\rho g}{r^2}(r - r_0)$$

where subscript 0 denotes a value at the surface and the other quantities are evaluated at the bottom ρ level.

Step 5. Form and solve the Helmholtz equation given by

$$\begin{aligned} - \quad & \kappa \rho \Pi \tfrac{\Delta t}{\rho} \delta_\eta \theta \left[\overline{\left(\tfrac{\tilde{\rho}^r w}{\delta_\eta r} \right)}^r + \overline{\left(\tfrac{\tilde{\rho}^r \alpha_2}{\delta_\eta r G} R_3^* - \Delta t \alpha_w C_p \theta \delta_r \left(\tfrac{\kappa \Pi p'}{p} \right) \right)}^r \right] \\ - \quad & \kappa \overline{\theta}^r \Pi \tfrac{\Delta t}{\delta_\eta r} \left[\delta_\eta \left(\tilde{\rho}^r (\dot{\eta} \delta_\eta r) + \tfrac{\alpha_2}{G} \left(R_3^* - \Delta t \alpha_w C_p \theta \delta_r \left(\tfrac{\kappa \Pi p'}{p} \right) \right) \right) \right] \\ + \quad & \kappa(\kappa - 1) \rho \overline{\theta}^r \Pi \tfrac{p'}{p} \\ = \quad & -(\kappa \rho \overline{\theta}^r \Pi - \tfrac{\rho r^2}{C_p} + \overline{R_4 - S_4}^r) \end{aligned} \tag{1.12}$$

where

$$G = \left(1 - \Delta t^2 \alpha_2 \alpha_w C_p \delta_{2r} \theta \delta_r \Pi\right)$$

and

$$R_3^* = R_3 - \Delta t \alpha_w C_p R_4 \delta_r \Pi$$

The derivation of the Helmholtz equation can be found in Appendix A.

After solving this equation we calculate w' from

$$w'G = R_3^* - \Delta t \alpha_w C_p \theta \delta_r \left(\frac{\kappa \Pi p'}{p} \right) \tag{1.13}$$

Step 6 Calculate $\dot{\eta}_1$ to enable ρ^{n+1} to be calculated.

$$w_1 = w^n + \alpha_2 w'$$

$$\dot{\eta}_1 = \frac{w_1}{\delta_\eta r}$$

$$\rho^{n+1} = \rho^n - \frac{\Delta t}{\delta_\eta r} \left[\delta_\eta (\tilde{\rho}^r (\dot{\eta}_1 \delta_\eta r)) \right] \tag{1.14}$$

Step 7 Use w_1 to calculate a better estimate of the advective term for θ. The advection is performed on an estimated value of θ at time level $n + 1/2$ denoted θ_1 and given by

$$\theta_1 = \theta^n + 0.5 * R_4$$

where R_4 is used as an estimate of θ', see equation (A.11).

The semi-Lagrangian scheme uses w_1 as the advecting velocity and monotone cubic interpolation. Conservation is enforced on the advective increment.

$$\theta'' = \theta_{1d} - \theta_1 + R_4 - S_4 \tag{1.15}$$

The first two terms on the right-hand-side represent the updated advective increment. The other terms hold the forcing increment, in this case $R_4 - S_4 = Q$, in the full 3D model it would be equal to the physics increment.

Step 8 Add increments to θ, w and p to update values to time-level $n + 1$, the update to ρ was performed in step 6.

$$\theta^{n+1} = \theta^n + \theta''$$

$$w^{n+1} = w^n + w'$$

$$p^{n+1} = p^n + p'$$

2 Test Problems.

The test problems are performed on a vertical grid of 40 points spaced at 400m intervals, with the surface being at 0m and the upper boundary at 16Km. The initial conditions are

$$w = 0$$

$$\theta = 290.7K$$

$$\Pi = 1 - \frac{gr}{C_p\theta}$$

$$p = P_{ref}\Pi^{1/k}$$

$$\rho = \frac{pr^2}{R\theta\Pi}$$

so that the air is at rest in a neutrally stable atmosphere and the equation of state is satisfied. These initial conditions also ensure that R_3 and R_4 are initially zero. The time-weighting parameters α_2, α_4, α_5 and α_w are set equal to each other and are referred to in the following pages by the collective name α.

2.1 Test Problem 1. The Organ Pipe.

This test problem is similar to that performed by Golding 1994 [2]. Here we used a timestep of 60 seconds rather than the 30 seconds he used and we replaced his fractional mass source with a density source, which has a similar effect. This is included by adding an extra term to the right-hand-side of equation (1.14) of the form

$$+0.001\ \Delta t r^2$$

the factor r^2 coming from the fact that we are not using the true density but r^2 times it as our variable. This term must also be added to the right-hand-side of equations (A.8) to (A.10) and hence included in the Helmholtz equation (A.16) and

(1.12). The density perturbation is applied at level 10 only, as in Golding, and we begin by running with a perturbation of 0.001*timestep and with the time-weighing parameters, α, set to 0.7. The results of the vertical velocity profile for the first four timesteps and then after 50, 100, 150 and 200 timesteps are shown in figures 2 and 3 respectively. Comparing the vertical velocity profiles after 4 timesteps and 200 timesteps it can be seen that the final solution is obtained very quickly as these two profiles are almost identical. With the time-weighting set to 0.7 we obtain the underlying steady state solution very quickly and the transient resonant sound waves are so strongly damped that they do not appear in the solution. This agrees with the results of Golding for $\alpha = 0.7$. Figure 4 shows the vertical velocity profiles for timesteps 198, 199 and 200 overlaid. It is impossible to see any differences between them and a similar result can be seen in the middle profile of figure 2 in Golding. The underlying solution for the pressure should be a linear increase with time at all levels. To see this in the model we plot the pressure difference from the initial pressure values. Figure 5 shows the profile for timesteps 1 to 4 and figure 6 shows the profile for timesteps 50, 100, 150 and 200. As we found with the vertical velocity profile the pressure solution is very smooth, but unlike the vertical velocity the values continue to increase with time. This is as expected, since we are adding mass and not allowing it to be removed and agrees with the underlying solution.

We now run the same experiment but with $\alpha = 0.5$. The resulting vertical velocity profile for the first 4 timesteps is shown in figure 7 and after 50, 100, 150 and 200 timesteps in figure 8. Here we can see that the underlying steady state solution is not achieved very quickly and that there are transient resonant sound waves present. This is because we are no longer applying the severe damping produced by using $\alpha = 0.7$. From figure 8 we can see that it takes some considerable time for the underlying solution to establish itself. What is important is not that there are transient waves, which in the real solution there are, but that they do not grow with time, and hence the numerical procedure is stable. By comparing the solutions after 150 and 200 timesteps it can be seen that there is no evidence of any growth with time and hence the method is stable. Figure 9 shows the vertical velocity profile for timesteps 198, 199 and 200 overlaid on each other. This clearly shows the transient

waves but the waves are quite smooth and physically realistic in shape. It is also easy to see that they are oscillations on top of the underlying solution by comparing with figure 4. It is interesting to compare this result with that obtained by Golding and to do this we re-plot figure 9 but using the same scale as that of figure 2 in Golding, this is shown in figure 10. Our algorithm shows smaller magnitude and smoother, more physically realistic, transient waves whilst the solution in Golding looks more noisy and less stable. The pressure change profiles for the first four timesteps are shown in figure 11 and those for timesteps 50, 100, 150 and 200 in figure 12. Not surprisingly we again see considerable variation in the solution for the first few timesteps. However comparing the result for timestep 50 with that for $\alpha = 0.7$ in figure 6 we see that they are very similar. In fact the pressure solutions are almost identical and become more so as the number of timesteps increase. It is interesting to note that the pressure solution is not sensitive to the transient wave activity.

The final experiment is carried out with the same timestep and with $\alpha = 0.5$ but using a density increment ten times greater i.e. 0.01*timestep. This is an extreme value and would not occur in the real atmosphere it is equivalent to a temperature increment of 400k being introduced in to the system every timestep. In fact it represents almost a doubling of the density value at level 10 on each timestep since the initial value is 0.82. The pressure change graphs are not presented as they are similar in shape to those for the smaller perturbation but ten times greater in magnitude. The results for the vertical velocity for the first 4 timesteps is shown in figure 13, and after 50,100,150 and 200 timesteps in figure 14, with figure 15 showing the profiles for timesteps 198, 199 and 200 overlaid. The results resemble the profiles obtained using a density increment ten times smaller. The transient waves are present but showing no signs of growing with time. This shows that even with an unrealistic perturbation the model retains a stable solution.

2.2 Explicit Convection.

In the test problem we again use 40 vertical levels with a spacing of 400m but force the problem with a potential temperature increment of 0.01 times the timestep at

level 10. If the forcing was only applied on the first timestep then it is possible to describe the physical solution. The solution should be an initial expansion wave centred on the perturbation followed by convection. The convection should initially be only above the perturbation but extending down towards the ground as time increases. This stage with convection throughout the whole depth is the underlying solution for the case used here where the temperature perturbation is added every timestep. This is easily shown by running this case with a long timestep, for example 5 minutes. We show the vertical velocity profile obtained for the first 4 timesteps with a 6 second timestep in figure 16. The first timestep clearly shows the expansion wave. In the second timestep convection is taking place almost throughout the entire depth, there is a small negative value at level 2. In the third timestep there is convection throughout the entire depth. Beyond timestep 3 we have a more complicated picture with the transient waves superimposed on the underlying solution. The only conclusion we can draw from the later timesteps is that the solution remains stable. A similar picture is gained with a shorter timestep, 3 seconds, as shown in figure 17, but it is easier to see the change from expansion wave to convection throughout the depth of the atmosphere.

3 Conclusions and Recommendations.

3.1 Conclusions.

The results of the scheme when perturbed by a density increment shows no sign of growth with time of transient resonant sound waves, even when extreme conditions are used in the test. When a realistic density perturbation is used a stable physically possible solution is reached and increasing this perturbation linearly produces only a linear increase in the transient waves. The underlying steady state solution is reached more quickly as the time-weighting parameters, α, are increased from the desired value of 0.5 to 1.0. This is because the greater the value of α the more the transient waves are damped and for $\alpha = 0.7$ it is almost impossible to see any transient waves. The solution with $\alpha = 0.5$ has the transient waves and looks physically plausible. The transient waves for $\alpha = 0.5$ are smoother, smaller and

less noisy than those obtained by Golding [2] in a similar test problem for the old non-hydrostatic mesoscale model. This is important as α must be set to 0.5 in the scheme in order to satisfy certain conservation laws and to obtain second order accuracy in time.

The behaviour of the model using a temperature increment again showed no signs of growing wave amplitudes and produces a physically realistic simulation of explicit convection.

3.2 Recommendations.

1. The time-weighting parameters α_4, α_5 and α_w be replaced by one parameter as α_4 and α_5 are really α_w. See Appendix A.

2. The time-weighting parameters are all set to 0.5 as an initial estimate of the values to be used in two- and three-dimensional simulations. They may need revising for stability requirements when running in more than the one-dimension used here.

3. In Appendix A it is noted that some of the terms neglected in forming the Helmholtz equation could be included easily. It may be worth investigating the impact of including those terms.

Bibliography

[1] M. J. P. Cullen, T. Davies and M. H. Mawson. *A proposed semi-implicit integration scheme for the Unified Model.* F. R. Division Working Paper No 154, version 7, 1994.

[2] B. W. Golding. *An efficient non-hydrostatic forecast model.* Meteorol. Atmos. Phys. **50**, pp 89–103, 1992.

[3] M. H. Mawson. *The proposed semi-Lagrangian advection scheme for the semi-implicit Unified model integration scheme.* F. R. Division Working Paper No 162, version 3, 1994.

Appendix A: Derivation of Helmholtz equation

We would like the model to satisfy the equation of state (1.4) at time level $n+1$ and when discretized it takes the following form

$$\kappa \Pi^{\kappa} \overline{\theta}^{r} \rho - \frac{p_{ref} r^2}{\kappa C_p} \Pi^{\frac{1}{\kappa}} = 0 \tag{A.1}$$

where all variables are at time level $n+1$. We now define

$$p' = p^{n+1} - p^n$$

with similar definitions for the other variables. Re-writing equation (A.1) with these definitions we get

$$\kappa \left(\frac{p+p'}{p_{ref}} \right)^{\kappa} (\overline{\theta + \theta'}^{r})(\rho + \rho') - \frac{r^2}{C_p}(p+p') = 0 \tag{A.2}$$

where all non primed variables are taken at time level n. For the rest of this derivation all variables are at time level n except where stated to the contrary. We now linearize equation (A.2) with respect to the primed variables. To do this we need to define the linearized form of

$$\left(\frac{p+p'}{p_{ref}} \right)^{\kappa}$$

This is done by writing this term as

$$\left(\frac{p}{p_{ref}} \right)^{\kappa} \left(1 + \frac{p'}{p} \right)^{\kappa}$$

and then expanding the second part of this expression to obtain

$$\left(\frac{p}{p_{ref}} \right)^{\kappa} \left(1 + \kappa \frac{p'}{p} + \frac{\kappa(\kappa-1)}{2} \left(\frac{p'}{p} \right)^2 + \ldots \right)$$

We now neglect terms in the expansion of order greater than 1 to obtain

$$\left(\frac{p}{p_{ref}} \right)^{\kappa} \left(1 + \kappa \frac{p'}{p} \right) \tag{A.3}$$

Using this definition and linearizing equation (A.2) we obtain

$$\kappa \rho \overline{\theta}^{r} \Pi - \frac{p r^2}{C_p} + \kappa \rho \overline{\theta'}^{r} \Pi + \kappa \rho' \overline{\theta}^{r} \Pi + \kappa(\kappa-1) \rho \overline{\theta}^{r} \Pi \frac{p'}{p} = 0 \tag{A.4}$$

We now need to write all the primed variables in terms of just one of them to obtain one equation in one unknown, rather than equation (A.4) which is one equation in

three unknowns. To do this we use the evolution equations for ρ, θ and w to obtain ρ', θ' and w' in terms of p'.

The discretized Eulerian form of the evolution equation for w is given by

$$\begin{aligned} w^{n+1} - w^n &= -\Delta t \quad [(w + \alpha_2 w')\delta_{2r}(w + \alpha_2 w') + g \\ &\qquad +(1 - \alpha_w)C_p\theta\delta_r\Pi + \alpha_w C_p\theta^{n+1}\delta_r\Pi^{n+1}\Big] \end{aligned} \tag{A.5}$$

Assuming that the semi-Lagrangian advection and the Eulerian advection of w differ little since we can then replace the Eulerian advection term at time level n with its semi-Lagrangian equivalent, and linearizing with respect to the primed variables we get

$$\begin{aligned} w' + \Delta t\alpha_2 w'\delta_{2r}w + \Delta t w\delta_{2r}(\alpha_2 w') & \\ + \Delta t\alpha_w C_p\theta'\delta_r\Pi + \Delta t\alpha_w C_p\theta\delta_r\left(\frac{\kappa\Pi p'}{p}\right) &= R_3 \end{aligned} \tag{A.6}$$

where we have used equation (A.3) to linearize the Exner pressure term at time level $n+1$, and R_3 is as defined in section 1.2, step 4. We note that in Cullen et al [1] α_w has been replaced by two different α's called α_4 and α_5. For consistency we should set $\alpha_w = \alpha_4 = \alpha_5$ and have only parameter. The current proposal also omits the two vertical advection terms in equation (A.6). The first term could be included easily but including the second would result in a significantly more complicated Helmholtz step. Following Cullen et al we neglect both. The θ' term is replaced using the approximation given by equation (A.13) to obtain

$$w'G = R_3^* - \Delta t\alpha_w C_p\theta\delta_r\left(\frac{\kappa\Pi p'}{p}\right) \tag{A.7}$$

where we have defined

$$G = \left(1 - \Delta t^2\alpha_2\alpha_w C_p\delta_{2r}\theta\delta_r\Pi\right)$$

and

$$R_3^* = R_3 - \Delta t\alpha_w C_p R_4\delta_r\Pi$$

The evolution equation for ρ is the continuity equation and the discrete form is

$$\rho^{n+1} = \rho^n - \frac{\Delta t}{\delta_\eta r}\left[\delta_\eta(\tilde{\rho}^r(\dot{\eta}_1\delta_\eta r))\right] \tag{A.8}$$

where

$$\dot{\eta}_1 = \frac{w_1}{\delta_\eta r}$$

and

$$w_1 = w^n + \alpha_2 w'$$

Using these definitions we obtain

$$\rho' = -\frac{\Delta t}{\delta_\eta r}\left[\delta_\eta(\tilde{\rho}^r(\dot{\eta}\delta_\eta r) + \alpha_2 w')\right] \tag{A.9}$$

and it just remains to substitute for w' in terms of p' in this equation to obtain

$$\rho' = -\frac{\Delta t}{\delta_\eta r}\left[\delta_\eta\left(\tilde{\rho}^r(\dot{\eta}\delta_\eta r) + \frac{\alpha_2}{G}\left(R_3^* - \Delta t\alpha_w C_p\theta\delta_r\left(\frac{\kappa\Pi p'}{p}\right)\right)\right)\right] \tag{A.10}$$

The discretized Eulerian form of the evolution equation for θ is given by

$$\theta^{n+1} = \theta^n - \Delta t(w + \alpha_2 w')\delta_{2r}(\theta + 0.5\theta') + Q \tag{A.11}$$

where Q is the θ increment discussed in section 1.2, step 3. Assuming that the semi-Lagrangian advection and the Eulerian advection of θ differ little and linearizing with respect to the primed variables we get

$$\theta' = -\Delta t\alpha_2 w'\delta_{2r}\theta - \Delta t w\delta_{2r}(0.5\theta') + R_4 \tag{A.12}$$

where R_4 is as defined in section 1.2, step 3. The second term on the right-hand-side of equation (A.12) is currently omitted from the scheme described by Cullen et al [1]. It could be included as it stands but only at the cost of making the resulting Helmholtz significantly more complicated and expensive to solve. One alternative is to approximate this term by setting $\theta' = R_4$. This would be consistent with the update performed in section 1.2, step 7, where θ' is approximated by R_4. This alternative has not been investigated here and following Cullen et al we neglect this term to obtain,

$$\theta' = R_4 - \Delta t\alpha_2 w'\delta_{2r}\theta \tag{A.13}$$

This is not the form we require to substitute into equation (A.4) since it is $\overline{\theta'}^r$ that is required. For the conversion terms between potential and kinetic energy to cancel a particular form must be used for this quantity, see Appendix B for details, this form is

$$\rho\overline{\theta'}^r = -\Delta t\overline{\tilde{\rho}^r\dot{\eta}_1}^r\delta_\eta\theta \tag{A.14}$$

it just remains to substitute for w' in terms of p' in this equation to obtain

$$\overline{\theta'}^r = -\frac{\Delta t}{\rho}\delta_\eta\theta\left[\overline{\left(\frac{\tilde{\rho}^r w}{\delta_\eta r}\right)}^r + \overline{\left(\frac{\tilde{\rho}^r\alpha_2}{\delta_\eta r G}R_3^* - \Delta t\alpha_w C_p\theta\delta_r\left(\frac{\kappa\Pi p'}{p}\right)\right)}^r\right] \tag{A.15}$$

The first term on the right-hand-side of equation (A.15) is the approximation to the first advection step for θ. Elsewhere in the derivation of the Helmholtz equation this is replaced by the semi-Lagrangian term, and hence would become S_4. However we cannot do this here and retain energy consistency. We thus note that if this term is not close to S_4 we have introduced a possibly significant inconsistency into the derivation. We still need to add the averaged forcing term to this equation and thus

$$\overline{R_4 - S_4}^r$$

is added to the right-hand-side of equation (A.15). Substituting equations (A.10) and (A.15) into equation (A.4) we obtain the Helmholtz equation

$$\begin{aligned}
- \quad & \kappa\rho\Pi\tfrac{\Delta t}{\rho}\delta_\eta\theta\left[\overline{\left(\tfrac{\tilde{\rho}^r w}{\delta_\eta r}\right)}^r + \overline{\left(\tfrac{\tilde{\rho}^r\alpha_2}{\delta_\eta r G}R_3^* - \Delta t\alpha_w C_p\theta\delta_r\left(\tfrac{\kappa\Pi p'}{p}\right)\right)}^r\right] \\
- \quad & \kappa\overline{\theta}^r\Pi\tfrac{\Delta t}{\delta_\eta r}\left[\delta_\eta\left(\tilde{\rho}^r(\dot{\eta}\delta_\eta r) + \tfrac{\alpha_2}{G}\left(R_3^* - \Delta t\alpha_w C_p\theta\delta_r\left(\tfrac{\kappa\Pi p'}{p}\right)\right)\right)\right] \\
+ \quad & \kappa(\kappa-1)\rho\overline{\theta}^r\Pi\tfrac{p'}{p} \\
= \quad & -(\kappa\rho\overline{\theta}^r\Pi - \tfrac{pr^2}{C_p} + \overline{R_4 - S_4}^r)
\end{aligned} \tag{A.16}$$

Appendix B: Energy consistency

Energetic consistency requires that the balance terms between kinetic and potential energy balance. We begin by showing analytically that this consistency exists. In the 1D model the energies are defined by

$$PE = \int C_v T \rho \frac{\partial r}{\partial \eta} d\eta \tag{B.1}$$

$$\int C_v \theta \Pi \rho \frac{\partial r}{\partial \eta} d\eta \tag{B.2}$$

$$KE = \int \frac{1}{2} \rho w^2 \frac{\partial r}{\partial \eta} d\eta \tag{B.3}$$

The evolution equation for w is

$$\frac{\partial w}{\partial t} + \dot{\eta} \frac{\partial w}{\partial \eta} + g + \frac{r^2}{\rho} \frac{\partial p}{\partial r} = 0 \tag{B.4}$$

and for ρ is

$$\frac{\partial \rho}{\partial t} + \frac{1}{\partial r / \partial \eta} \left[\frac{\partial}{\partial \eta} \left(\rho \dot{\eta} \frac{\partial r}{\partial \eta} \right) \right] = 0 \tag{B.5}$$

so that the kinetic energy evolution equation is given by

$$\frac{\partial}{\partial t} \left(\frac{1}{2} \rho \frac{\partial r}{\partial \eta} w^2 \right) + \frac{\partial}{\partial \eta} \left(\frac{1}{2} \rho \frac{\partial r}{\partial \eta} w^2 \right) + \rho g w \frac{\partial r}{\partial \eta} + w r^2 \frac{\partial r}{\partial \eta} \frac{\partial p}{\partial r} = 0 \tag{B.6}$$

where the last term on the left hand side is the conversion term. The rate of change of internal energy is given by

$$\frac{\partial}{\partial t} \left(C_v \Pi \theta \rho \frac{\partial r}{\partial \eta} \right) = \frac{r^2 C_v}{R} \frac{\partial r}{\partial \eta} \frac{\partial p}{\partial t} \tag{B.7}$$

where we have used the equation of state

$$r^2 p = \rho R \Pi \theta \tag{B.8}$$

The evolution equation for the equation of state is

$$\Pi \theta \frac{\partial \rho}{\partial t} + \rho \Pi \frac{\partial \theta}{\partial t} + \rho \theta (\kappa - 1) \frac{\Pi}{p} \frac{\partial p}{\partial t} = 0 \tag{B.9}$$

and for θ

$$\frac{\partial \theta}{\partial t} + \dot{\eta} \frac{\partial \theta}{\partial \eta} = 0 \tag{B.10}$$

and substituting the evolution equation for θ, (B.10), and for ρ, (B.5) into equation (B.9) gives

$$\frac{\rho(\kappa - 1)\theta}{p} \frac{\partial r}{\partial \eta} \frac{\partial p}{\partial t} = \frac{\partial}{\partial \eta} \left(\rho \dot{\eta} \theta \frac{\partial r}{\partial \eta} \right) \tag{B.11}$$

Therefore the rate of change of internal energy is given by

$$\frac{r^2 C_v p}{R\rho(\kappa-1)\theta}\frac{\partial}{\partial\eta}\left(\rho\dot{\eta}\theta\frac{\partial r}{\partial\eta}\right) \tag{B.12}$$

which is

$$-C_p\Pi\frac{\partial}{\partial\eta}\left(\rho\dot{\eta}\theta\frac{\partial r}{\partial\eta}\right) \tag{B.13}$$

Using the equation of state to write this in terms of pressure gives

$$-\frac{\Pi}{\kappa}\frac{\partial}{\partial\eta}\left(\frac{r^2 wp}{\Pi}\right) \tag{B.14}$$

noting that

$$w=\dot{\eta}\frac{\partial r}{\partial\eta} \tag{B.15}$$

Equation (B.14) is equal to

$$-\frac{r^2 p}{\kappa}\frac{\partial w}{\partial\eta}+\frac{r^2 w(\kappa-1)}{\kappa}\frac{\partial p}{\partial\eta}-\frac{wp}{\kappa}\frac{\partial r^2}{\partial\eta} \tag{B.16}$$

Adding this to the conversion term for KE gives

$$-\frac{1}{\kappa}\frac{\partial}{\partial\eta}\left(r^2 pw\right) \tag{B.17}$$

which when integrated from the surface to the top of the model gives zero since $w=0$ at the surface and top of the model.

The proof for the discrete case goes as follows;

Note that the primed variables represent the difference between time levels $n+1$ and n.

The discrete evolution equation for ρ is given by

$$\rho'=-\frac{\Delta t}{\delta_\eta r}\left[\delta_\eta(\tilde{\rho}^r(\dot{\eta}_1\delta_\eta r))\right] \tag{B.18}$$

with

$$w_1=w^n+\alpha_2 w'$$

$$\dot{\eta}_1=\frac{w_1}{\delta_\eta r}$$

and the discrete equation of state is

$$r^2 p=\rho R\Pi\overline{\theta}^r \tag{B.19}$$

The evolution equation for the equation of state is given by

$$\Pi\overline{\theta}^r \frac{\rho'}{\Delta t} + \rho\Pi\frac{\overline{\theta'}^r}{\Delta t} + \rho\overline{\theta}^r(\kappa-1)\frac{\Pi}{p}\frac{p'}{\Delta t} = 0 \tag{B.20}$$

Substituting for ρ' in equation (B.20) gives

$$-\frac{\Pi\overline{\theta}^r}{\delta_\eta r}\delta_\eta(\tilde{\rho}^r w_1) + \rho\Pi\frac{\overline{\theta'}^r}{\Delta t} + \rho\overline{\theta}^r(\kappa-1)\frac{\Pi}{p}\frac{p'}{\Delta t} = 0 \tag{B.21}$$

The approximation to the conversion term in the kinetic energy evolution equation is

$$w_1 r^2 \delta_\eta r \delta_r p \tag{B.22}$$

noting that it is $\dot{\eta}_1$ and hence w_1 that appears in the ρ evolution equation (B.18) and also that the advecting velocity in the w evolution equations should also be w_1. Equation (B.22) becomes

$$w_1\tilde{\rho}^r C_p\theta\delta_\eta r\delta_r\Pi \tag{B.23}$$

when the vertical pressure gradient term is evaluated in the model. The approximation to the internal energy change is

$$\frac{C_v}{\Delta t}\left(\overline{\theta}^r\Pi\rho\right)'\delta_\eta r \tag{B.24}$$

or equivalently

$$\frac{1-\kappa}{\kappa\Delta t}r^2 p'\delta_\eta r \tag{B.25}$$

In order to prove consistency of the energy conversion it is necessary to set

$$\frac{\overline{\theta'}^r}{\Delta t} = -\frac{\overline{\tilde{\rho}^r\dot{\eta}_1}^r}{\rho}\delta_\eta\theta \tag{B.26}$$

Note that this provides via equation (B.20) a definite relationship between ρ' and p', and also that equation (B.26) is not used to update θ. Substituting equation (B.26) into equation (B.21) gives

$$-\frac{\Pi\overline{\theta}^r}{\delta_\eta r}\delta_\eta(\tilde{\rho}^r w_1) - \Pi\frac{\overline{\tilde{\rho}^r w_1}^r}{\delta_\eta r}\delta_\eta\theta + \rho\overline{\theta}^r(\kappa-1)\frac{\Pi}{p}\frac{p'}{\Delta t} = 0 \tag{B.27}$$

and substituting this into equation (B.25) and using the equation of state gives

$$-C_p\Pi\left(\overline{\theta}^r\delta_\eta(\tilde{\rho}^r w_1) + \overline{\tilde{\rho}^r w_1}^r\delta_\eta\theta\right) \tag{B.28}$$

The conversion terms in the evolution equations for KE and PE should be equal and opposite when integrated. This means that equations (B.23) and (B.28) should be

equal. Noting that these quantities are at different levels in the vertical, the first term in equation (B.28) is subtracted from equation (B.23). Multiplying by $\delta\eta$ and summing gives, after significant algebra,

$$\sum_i \Pi_i C_p (\delta_\eta \theta)_i (\tilde{\rho}^T w_1)_i \tag{B.29}$$

which cancels the second term in equation (B.28) as required, when it is multiplied by $\delta\eta$ and summed.

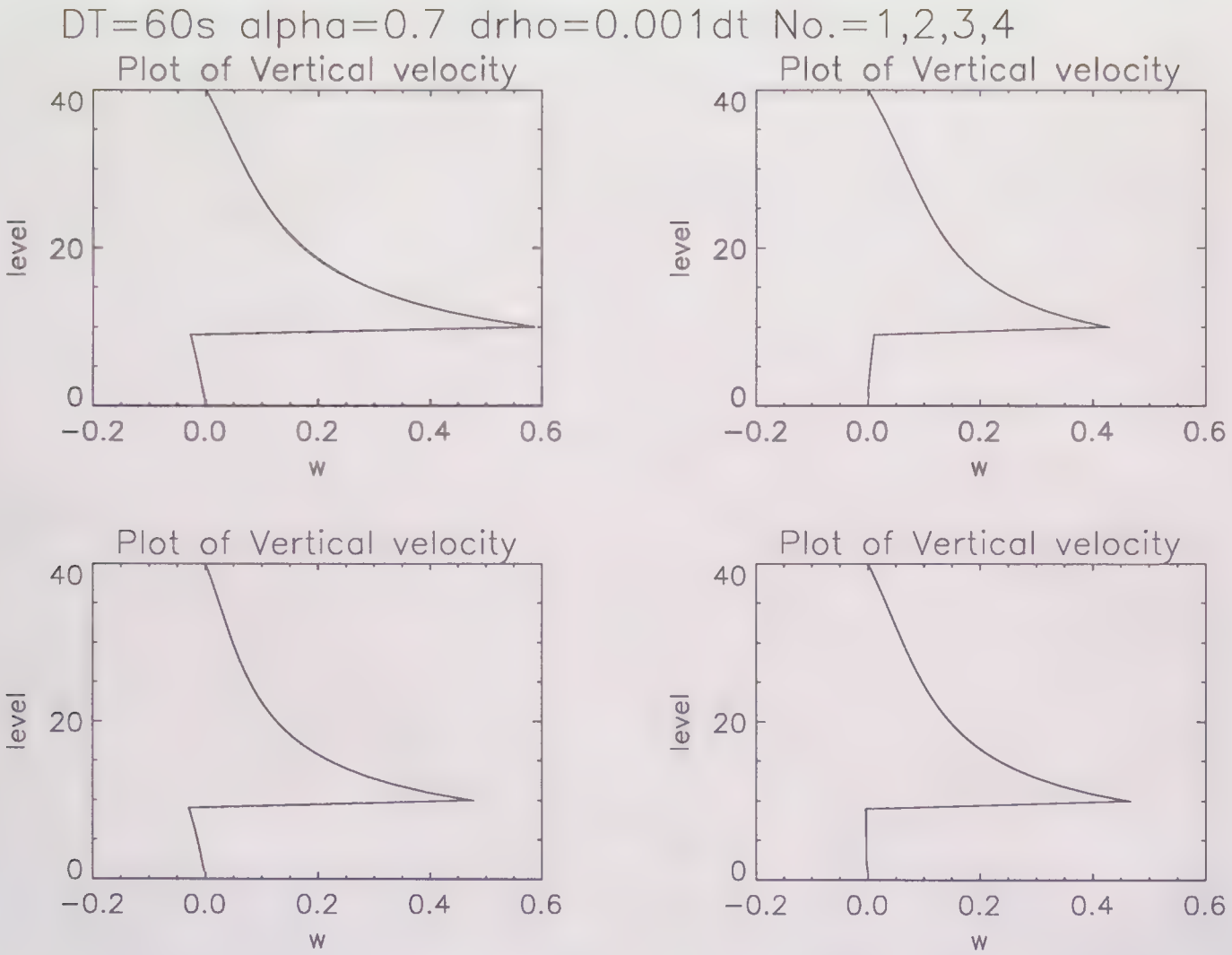
DT=60s alpha=0.7 drho=0.001dt No.=1,2,3,4
Plot of Vertical velocity
level
w
40
20
0
−0.2
0.0
0.2
0.4
0.6

Figure 2:

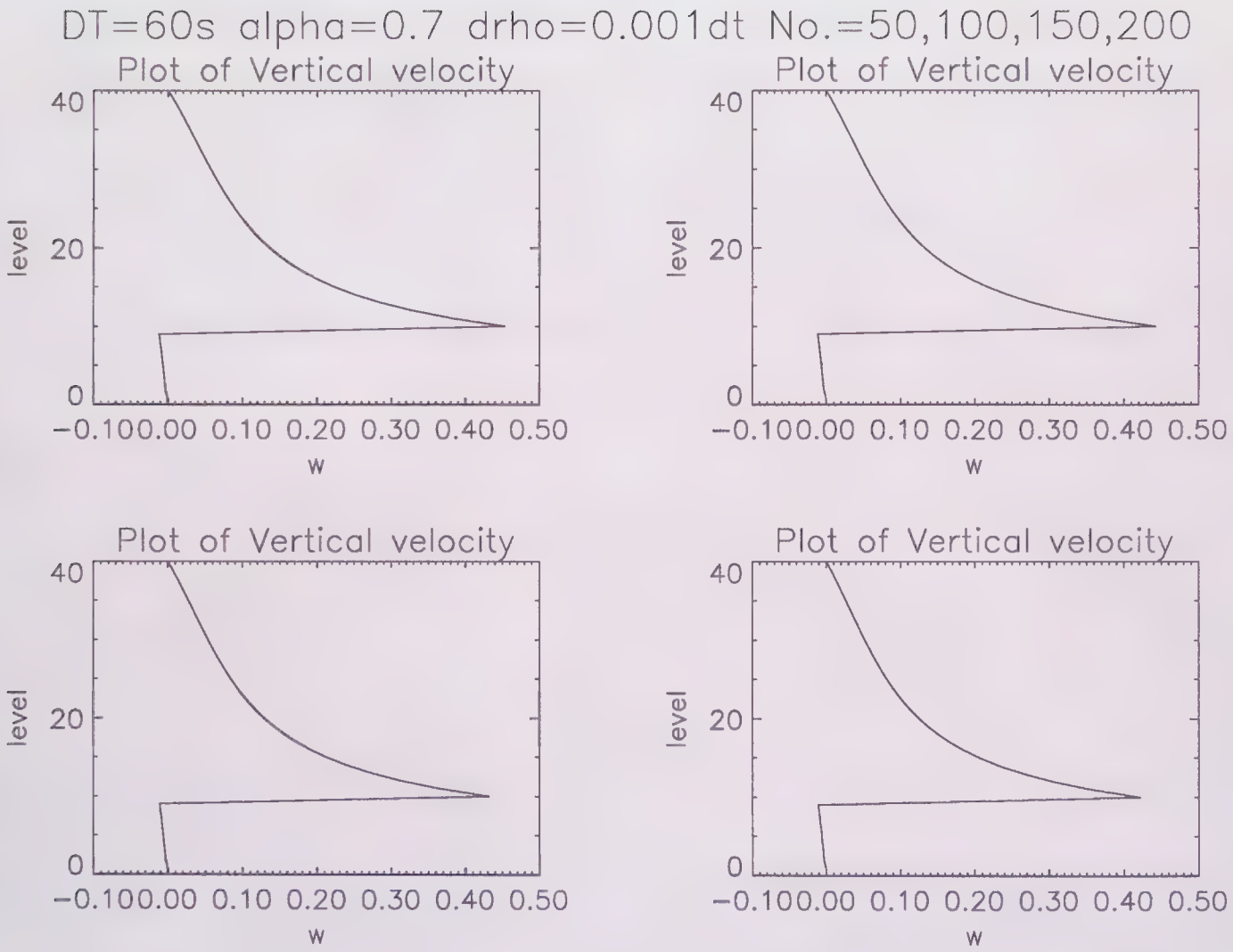
DT=60s alpha=0.7 drho=0.001dt No.=50,100,150,200
Plot of Vertical velocity
level
40
20
0
−0.100.00 0.10 0.20 0.30 0.40 0.50
w
Plot of Vertical velocity
level
40
20
0
−0.100.00 0.10 0.20 0.30 0.40 0.50
w
Plot of Vertical velocity
level
40
20
0
−0.100.00 0.10 0.20 0.30 0.40 0.50
w
Plot of Vertical velocity
level
40
20
0
−0.100.00 0.10 0.20 0.30 0.40 0.50
w

Figure 3:

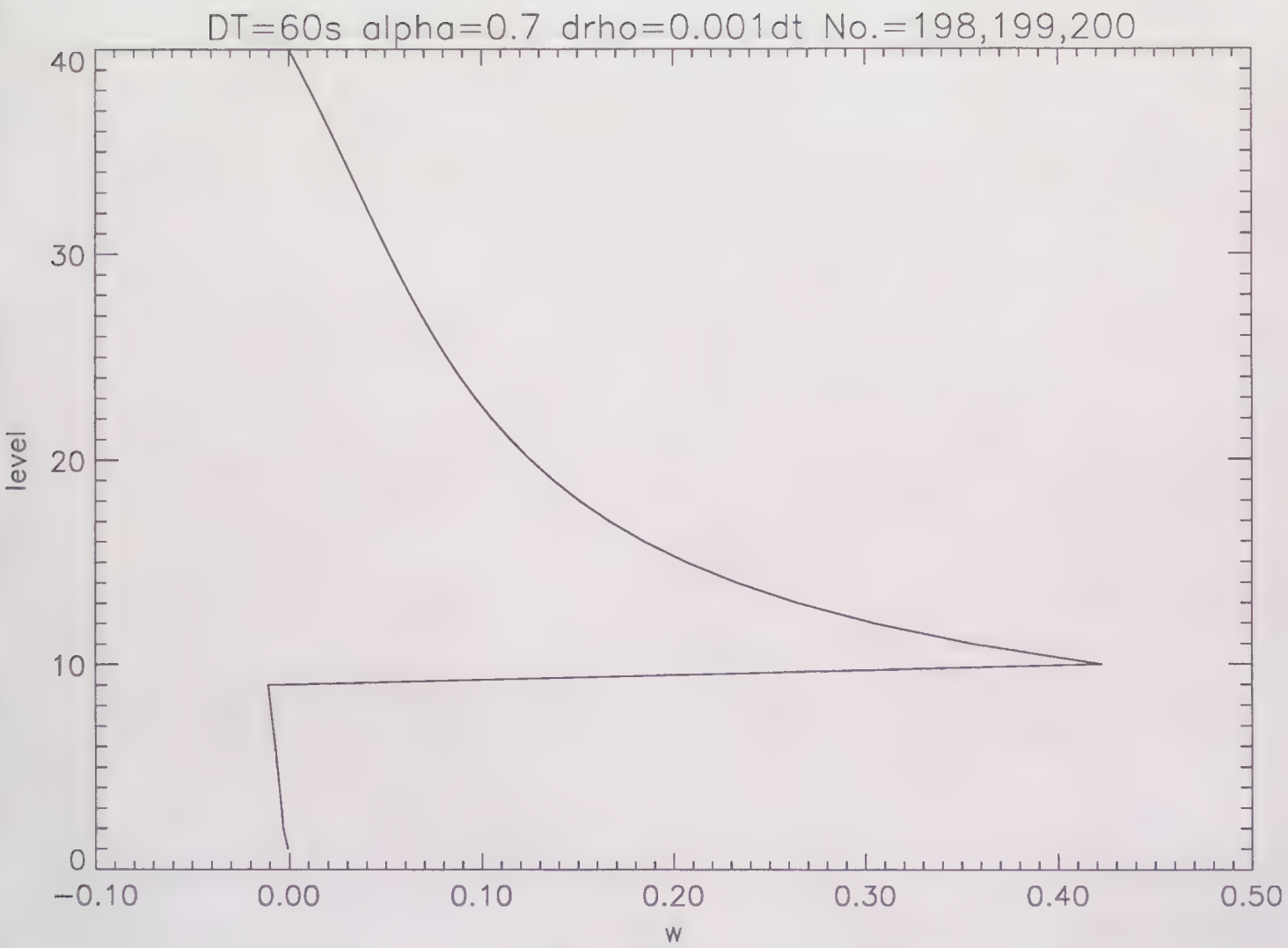
DT=60s alpha=0.7 drho=0.001dt No.=198,199,200
level
w
40
30
20
10
0
−0.10
0.00
0.10
0.20
0.30
0.40
0.50

Figure 4:

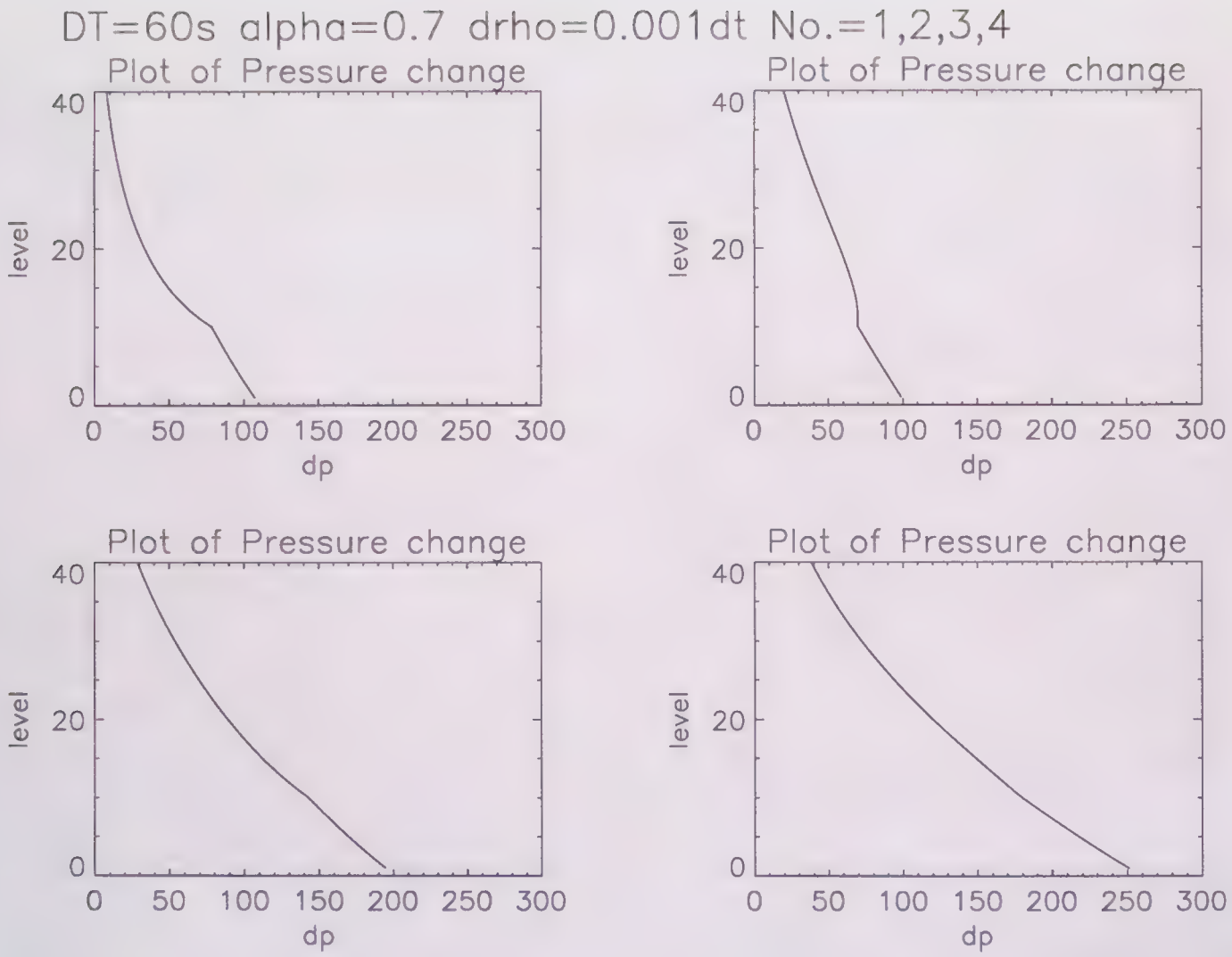
DT=60s alpha=0.7 drho=0.001dt No.=1,2,3,4
Plot of Pressure change
level
dp
0
20
40
0 50 100 150 200 250 300

Figure 5:

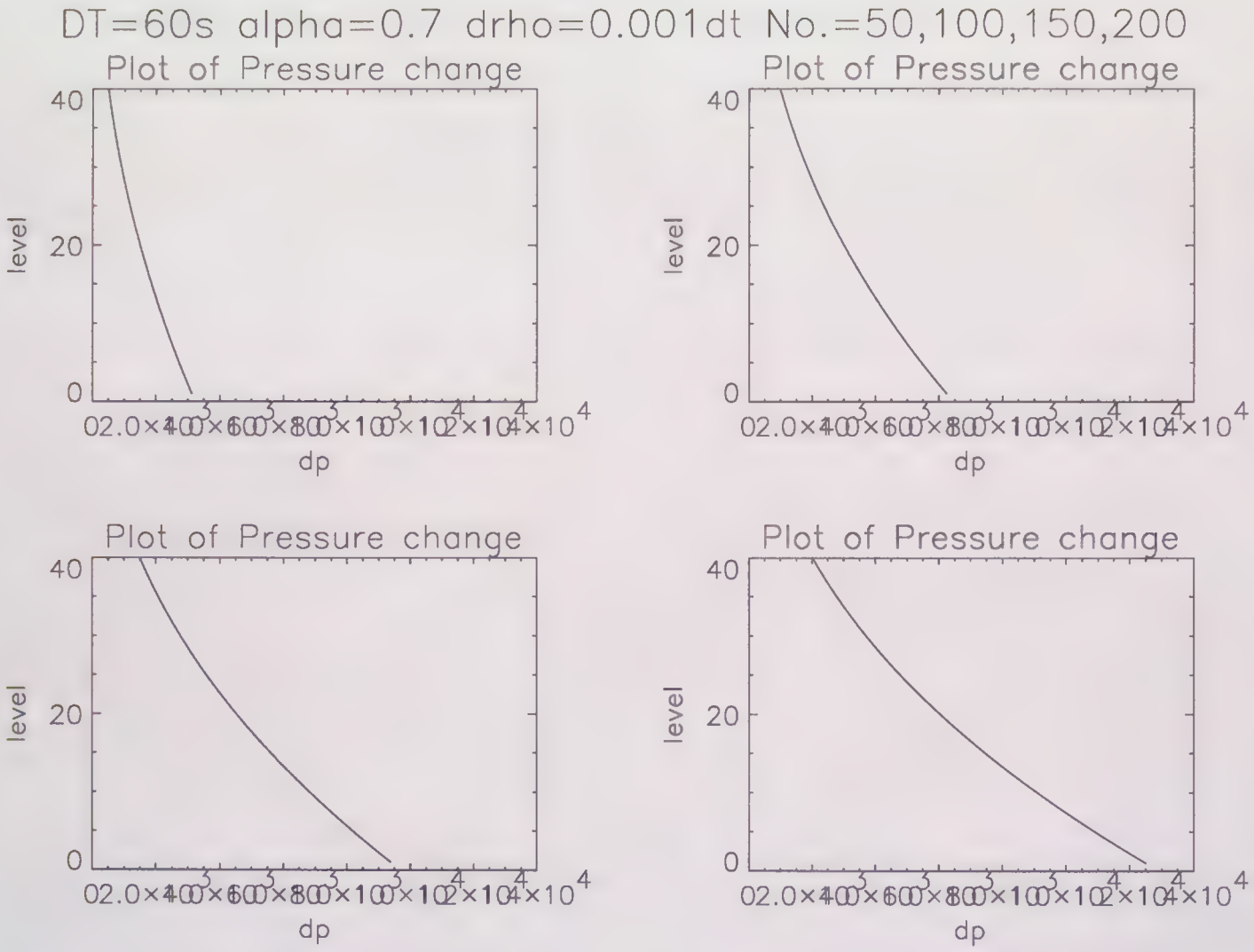
DT=60s alpha=0.7 drho=0.001dt No.=50,100,150,200
Plot of Pressure change
level
dp
Plot of Pressure change
level
dp
Plot of Pressure change
level
dp
Plot of Pressure change
level
dp

Figure 6:

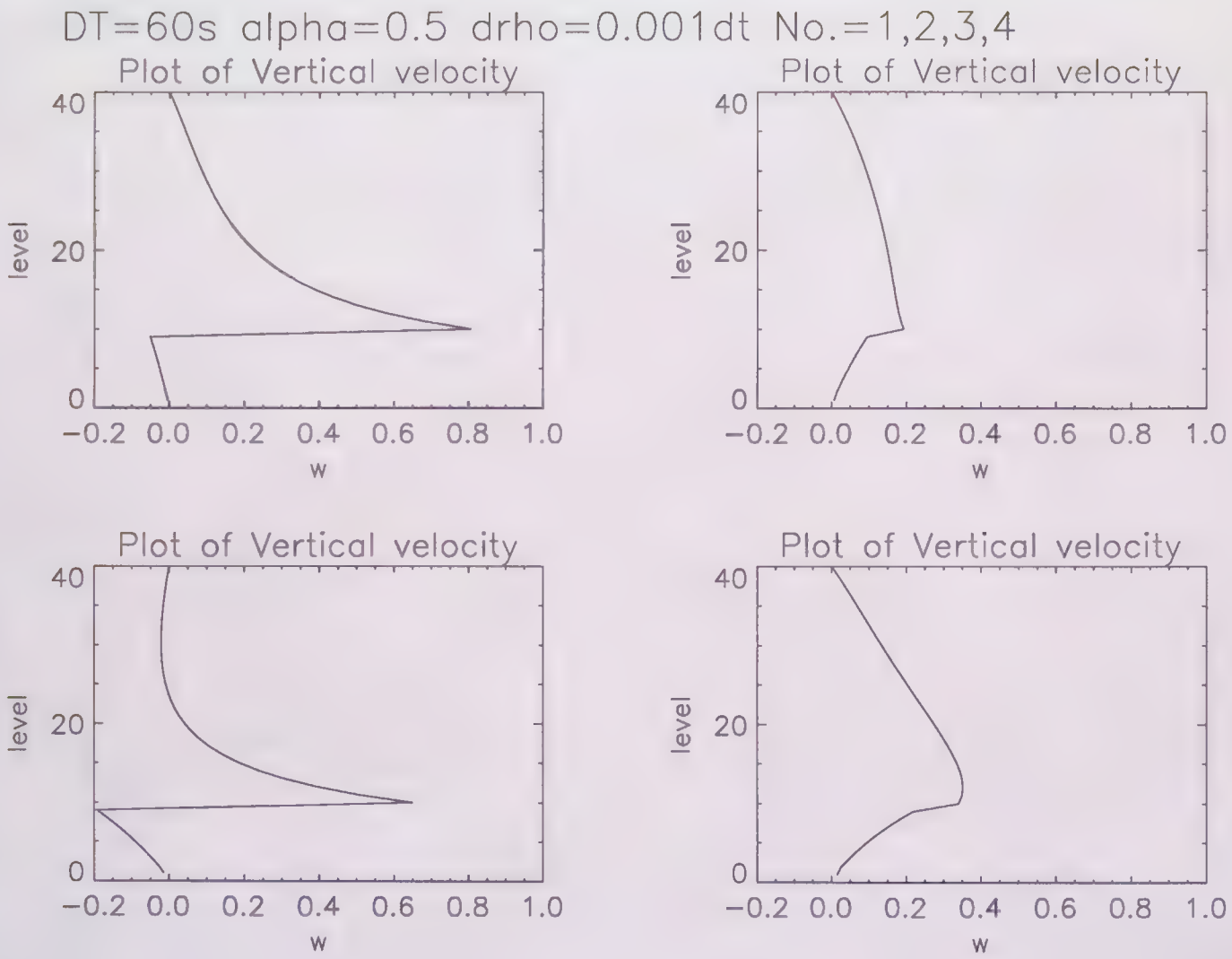
DT=60s alpha=0.5 drho=0.001dt No.=1,2,3,4
Plot of Vertical velocity
Plot of Vertical velocity
Plot of Vertical velocity
Plot of Vertical velocity
level
w
40
20
0
−0.2 0.0 0.2 0.4 0.6 0.8 1.0

Figure 7:

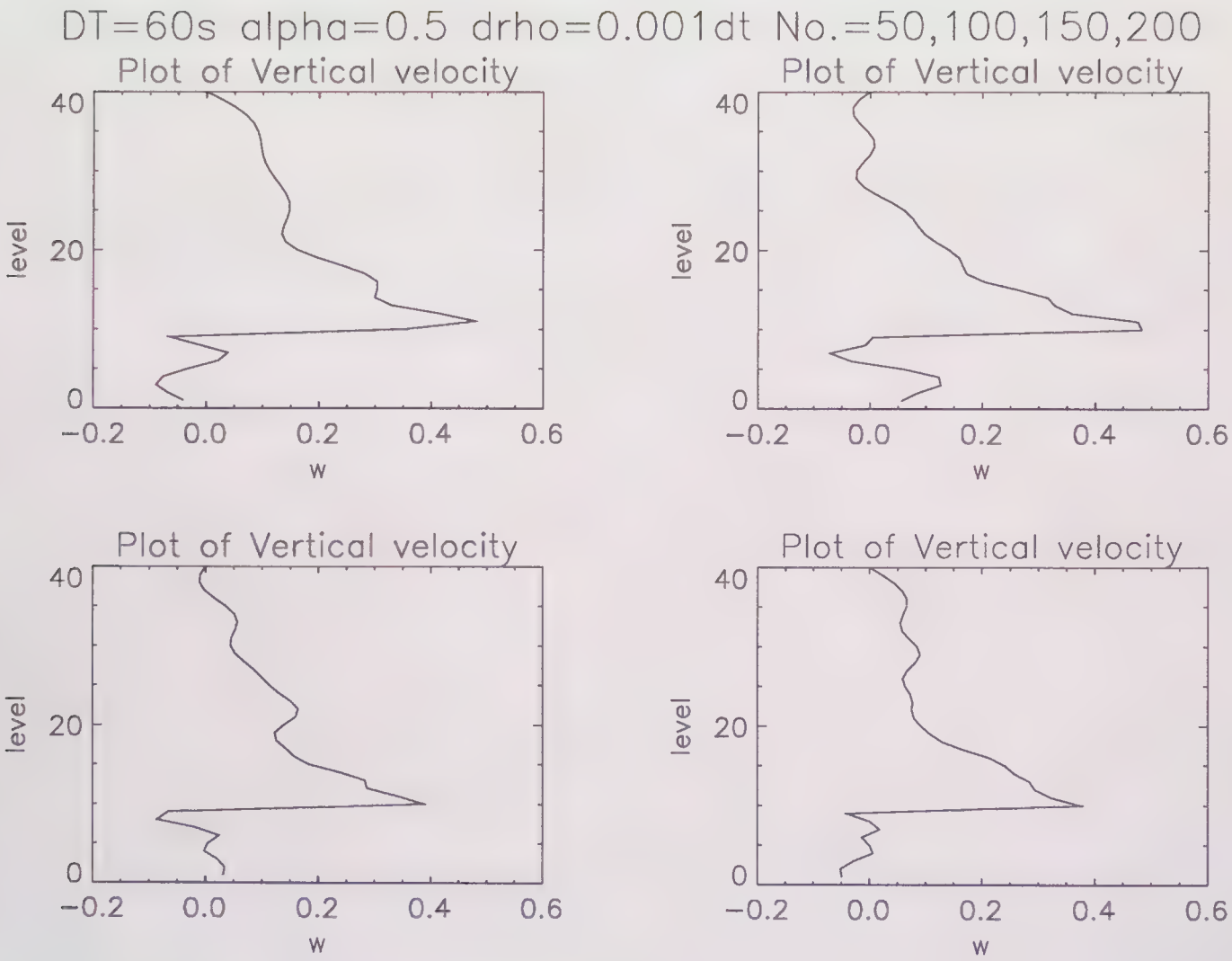
DT=60s alpha=0.5 drho=0.001dt No.=50,100,150,200
Plot of Vertical velocity
level
w
40
20
0
−0.2
0.0
0.2
0.4
0.6

Figure 8:

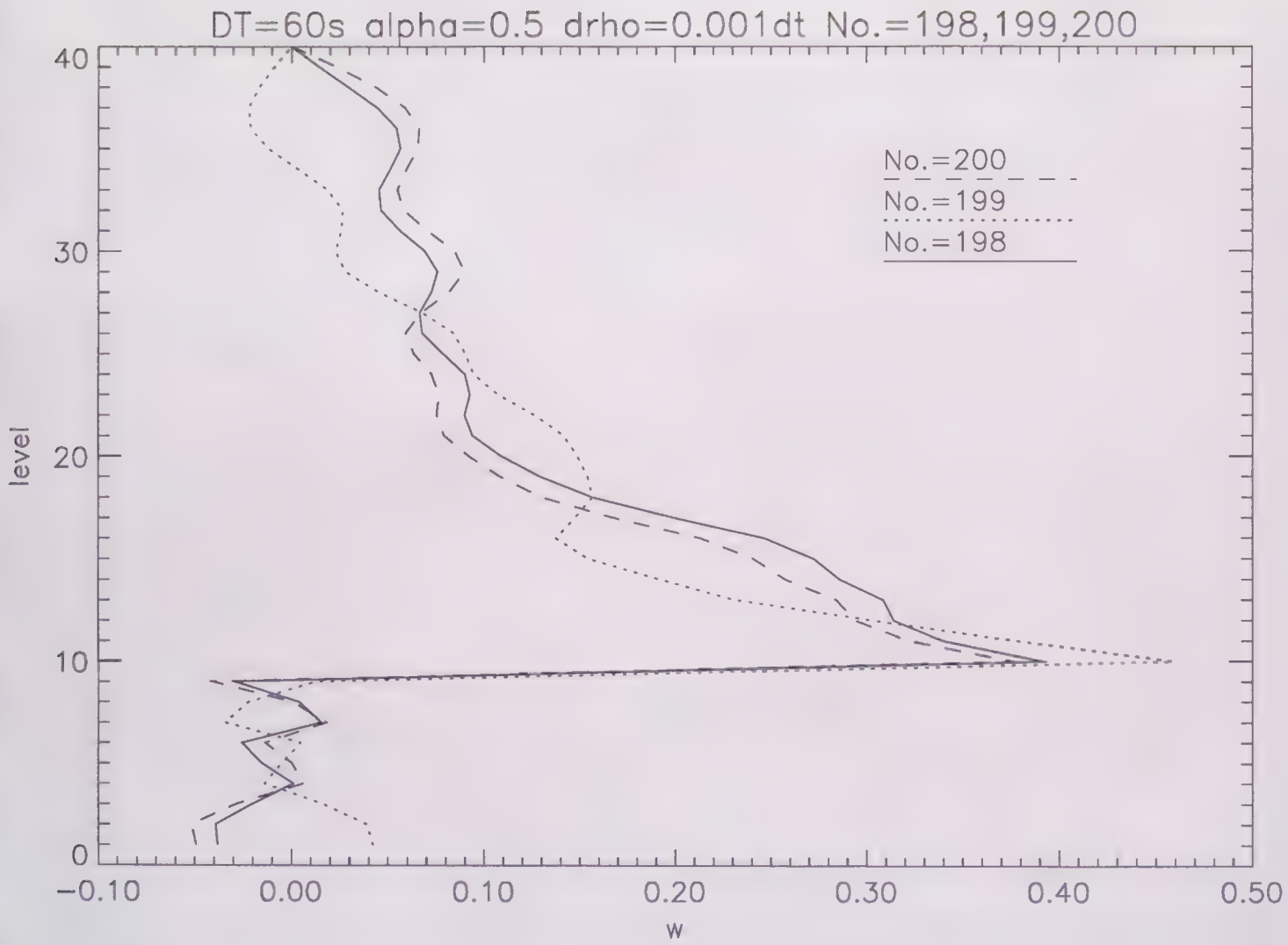
DT=60s alpha=0.5 drho=0.001dt No.=198,199,200
No.=200
No.=199
No.=198
level
w
40
30
20
10
0
−0.10
0.00
0.10
0.20
0.30
0.40
0.50

Figure 9:

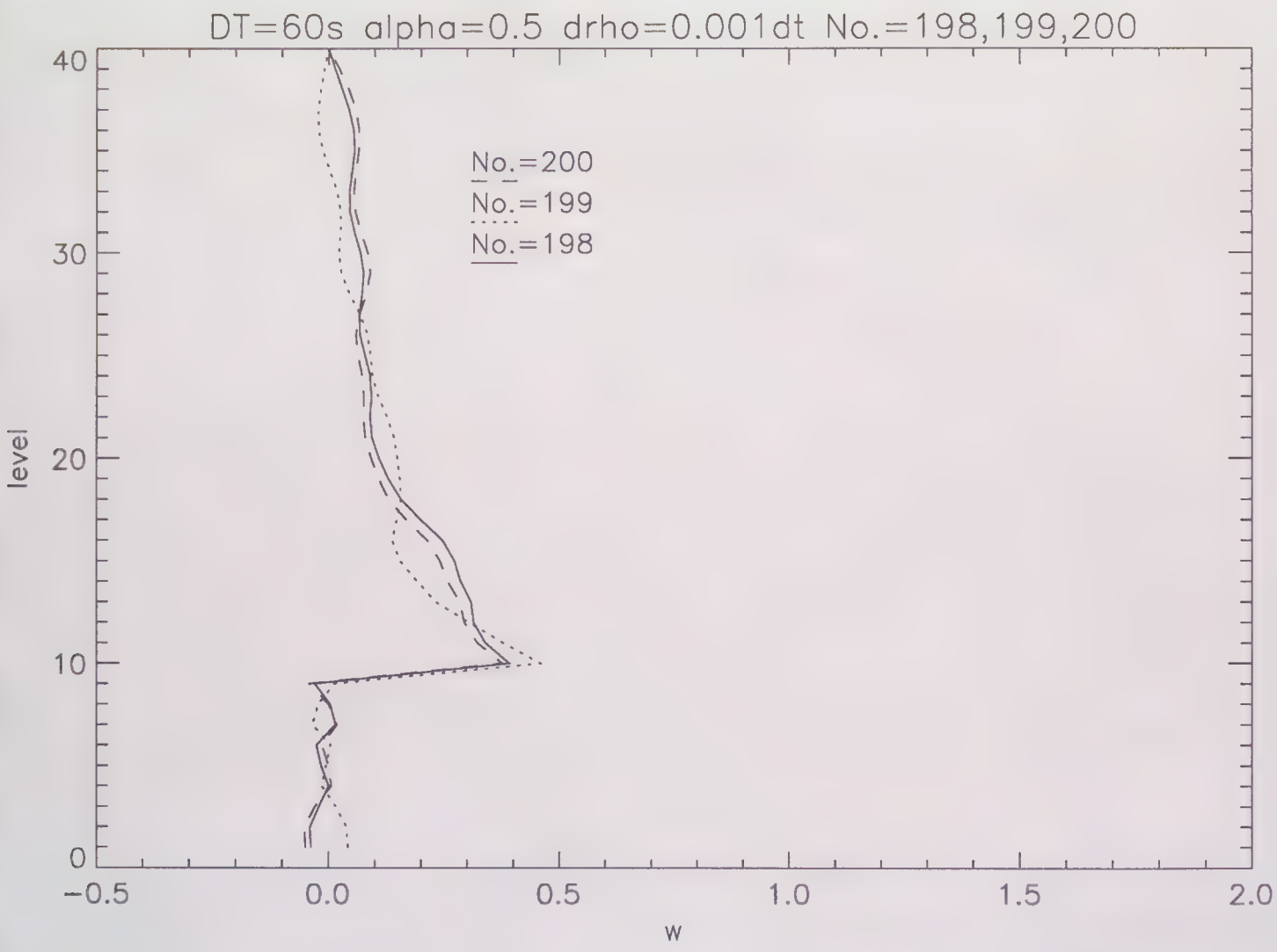
DT=60s alpha=0.5 drho=0.001dt No.=198,199,200
No.=200
No.=199
No.=198
level
w
40
30
20
10
0
−0.5
0.0
0.5
1.0
1.5
2.0

Figure 10:

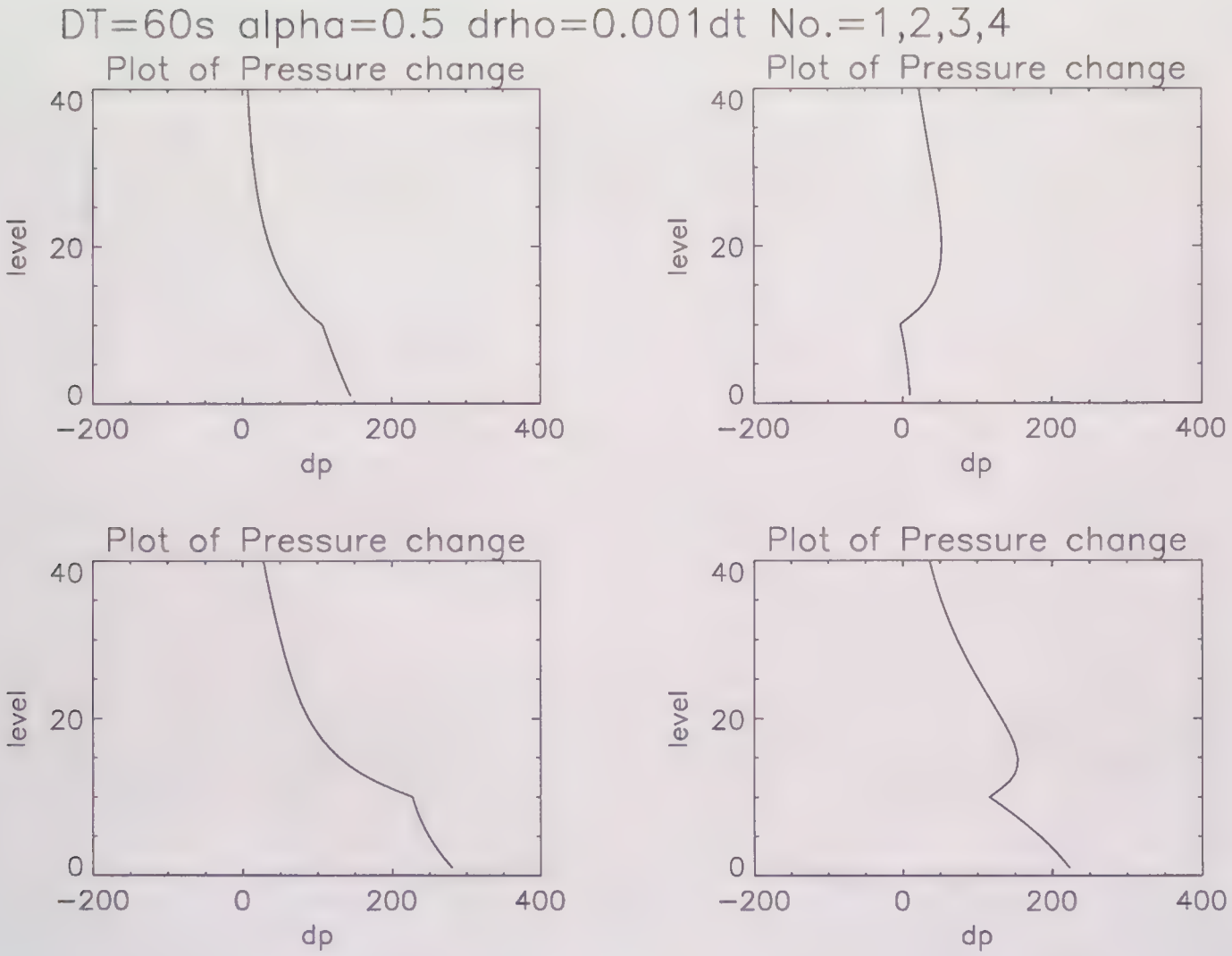
DT=60s alpha=0.5 drho=0.001dt No.=1,2,3,4
Plot of Pressure change
level
dp
40
20
0
−200
0
200
400

Figure 11:

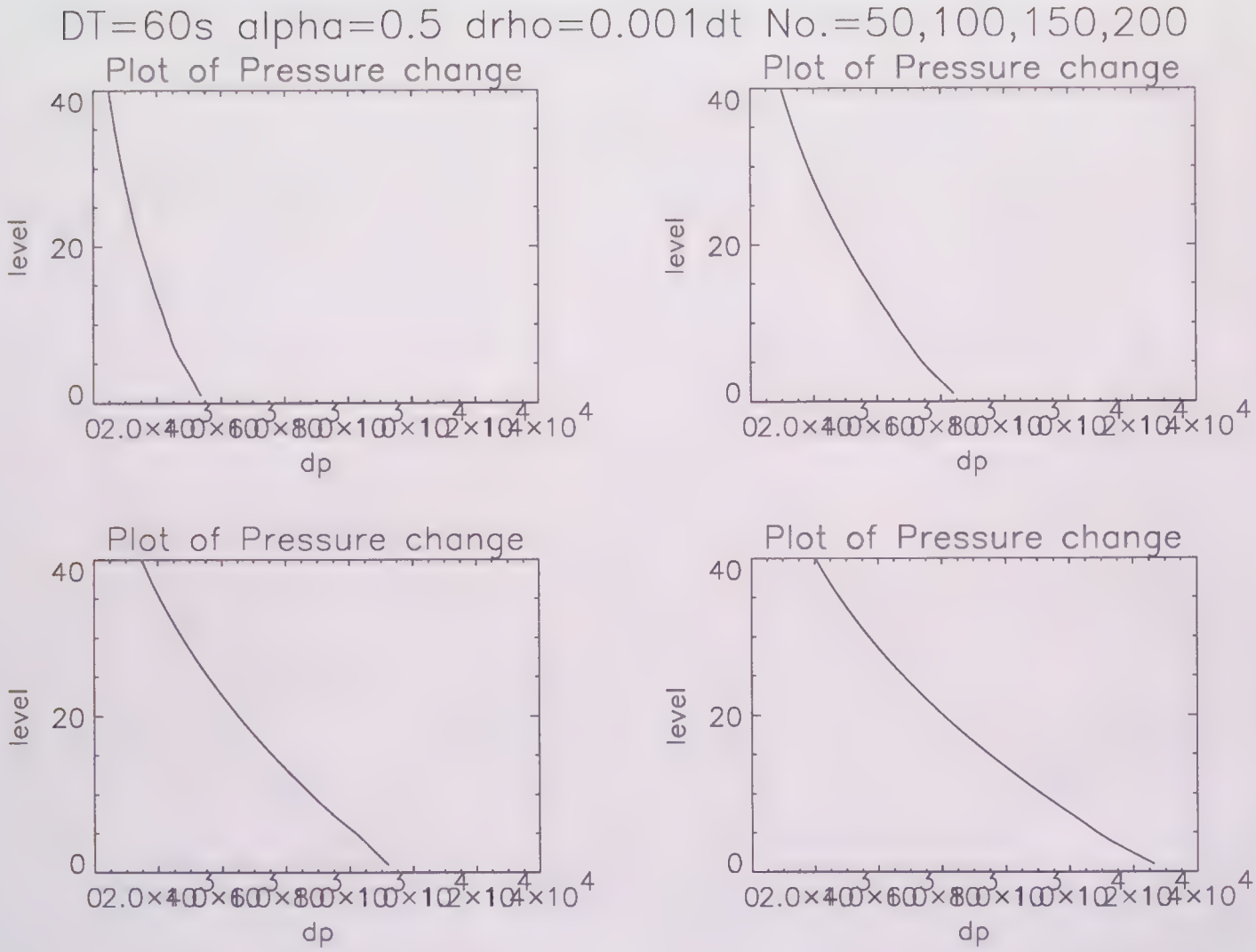
DT=60s alpha=0.5 drho=0.001dt No.=50,100,150,200
Plot of Pressure change
level
dp
Plot of Pressure change
level
dp
Plot of Pressure change
level
dp
Plot of Pressure change
level
dp

Figure 12:

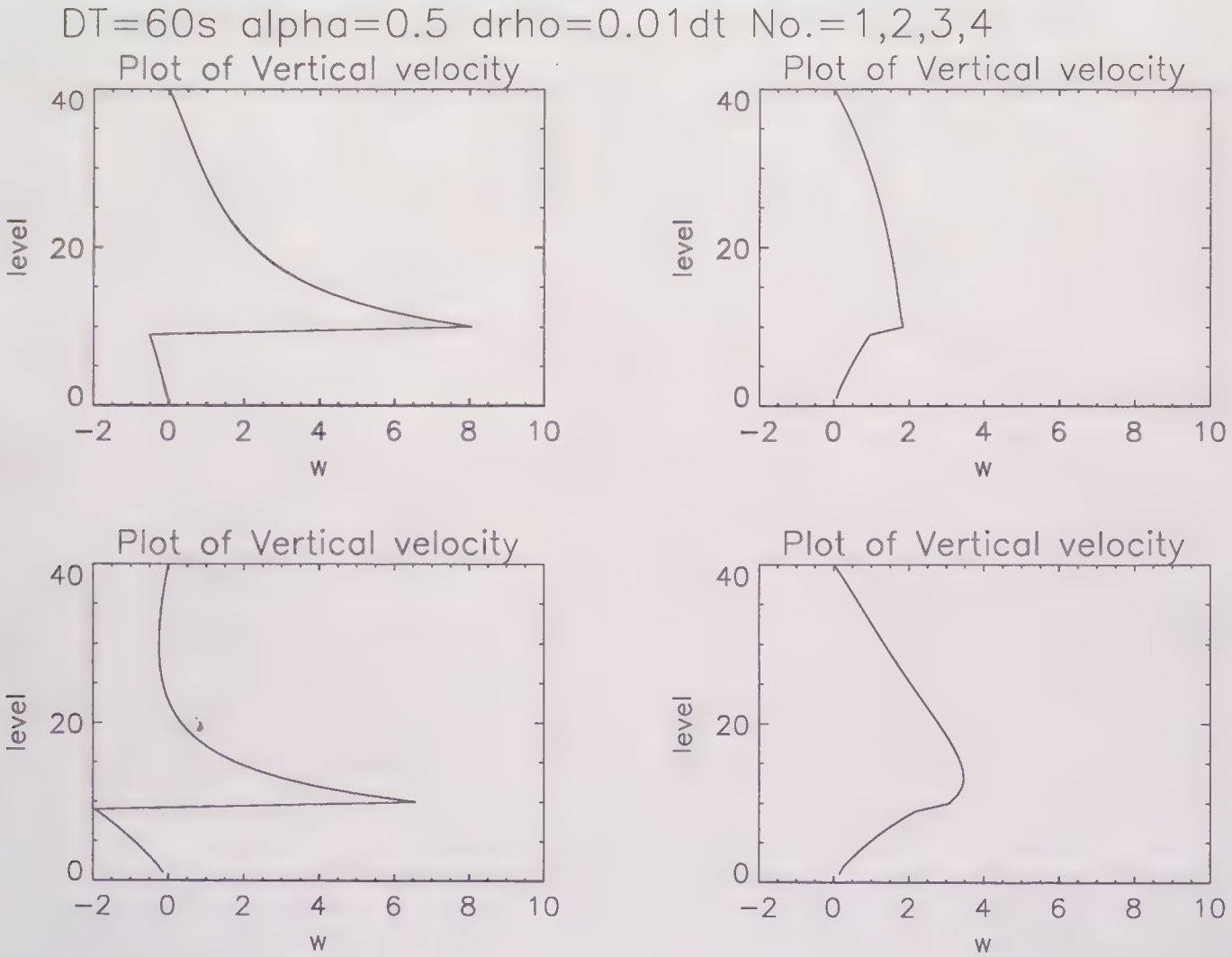
DT=60s alpha=0.5 drho=0.01dt No.=1,2,3,4
Plot of Vertical velocity
level
w
40
20
0
−2
0
2
4
6
8
10

Figure 13:

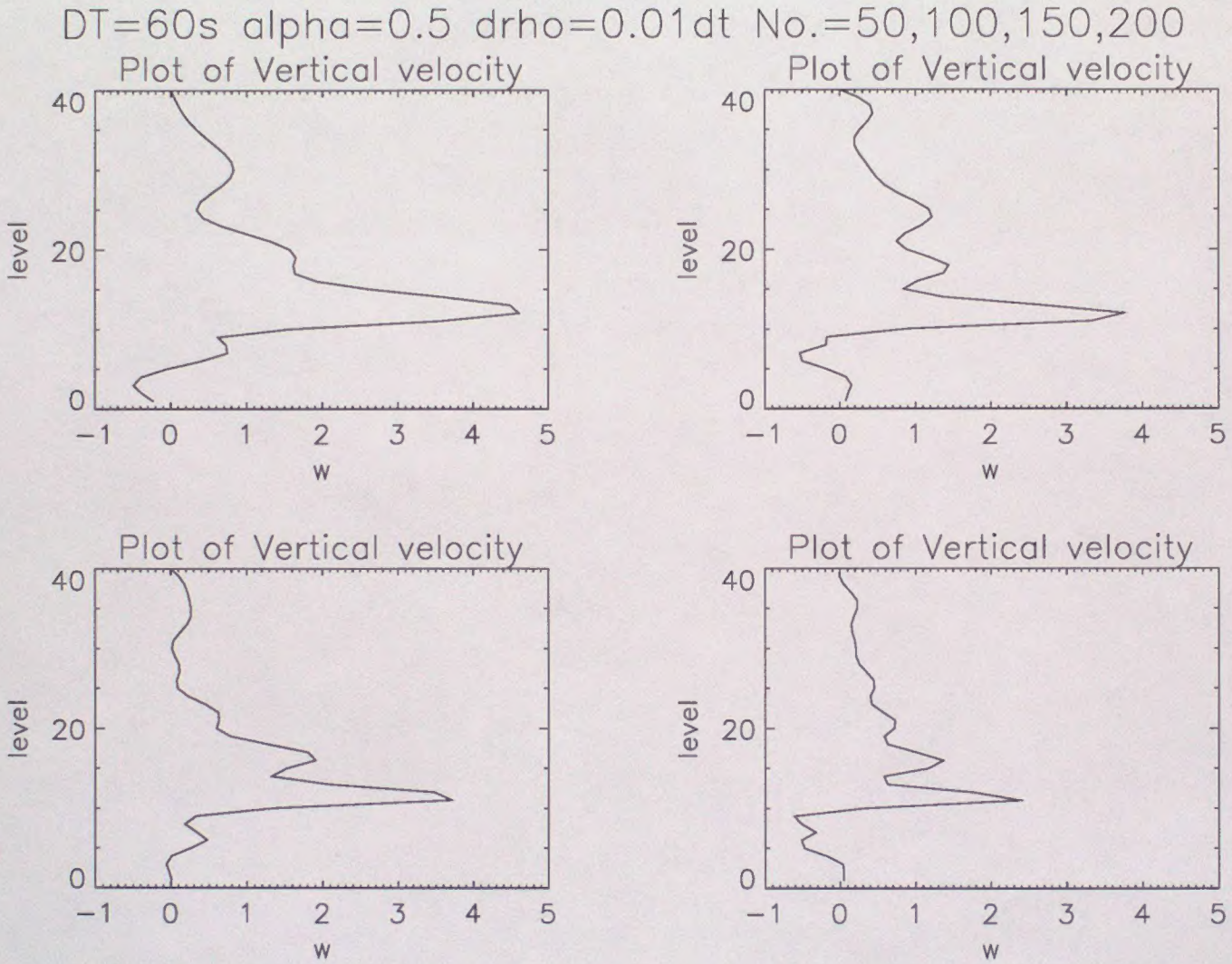
DT=60s alpha=0.5 drho=0.01dt No.=50,100,150,200
Plot of Vertical velocity
level
w
40
20
0
−1
0
1
2
3
4
5

Figure 14:

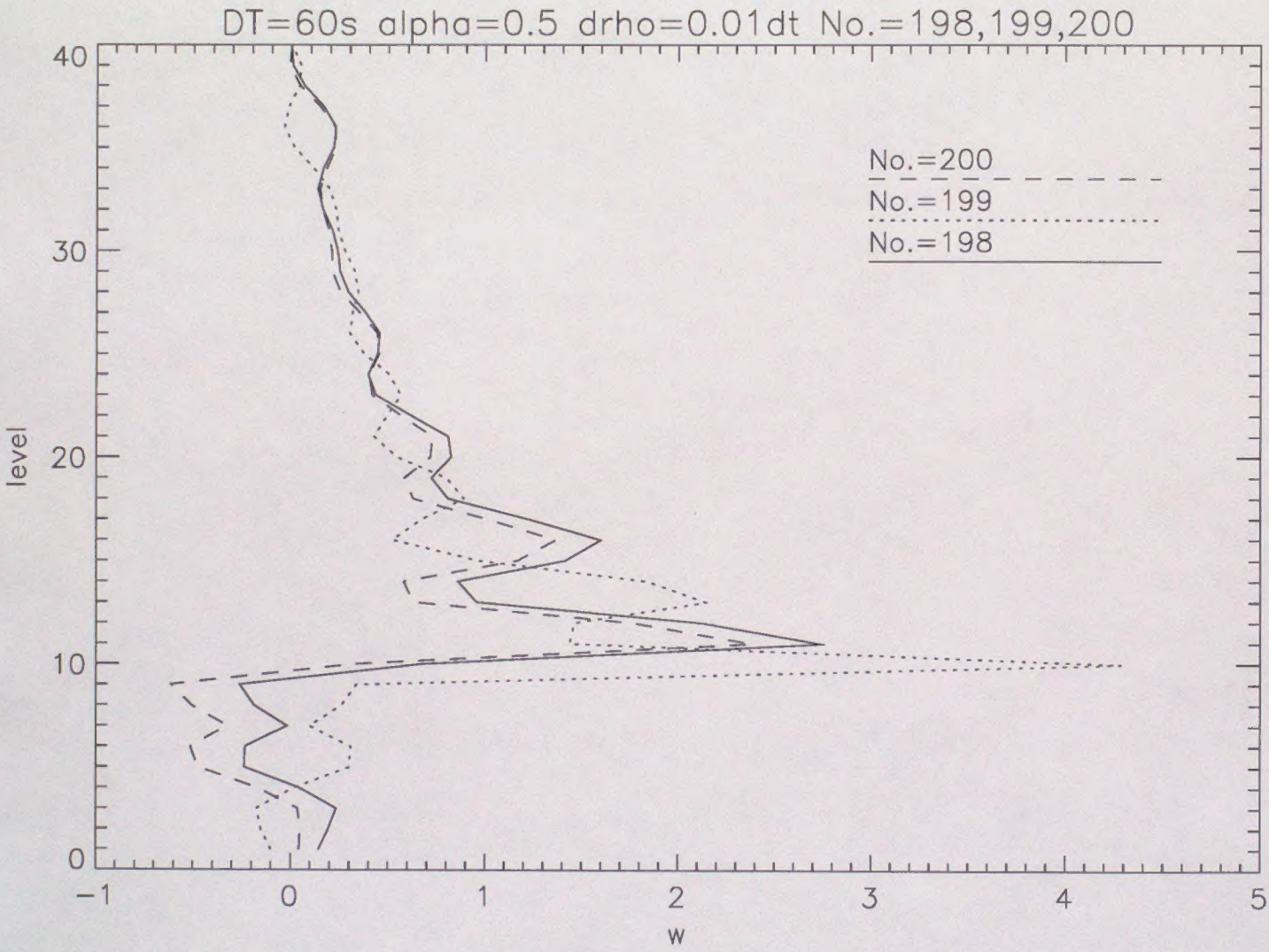
DT=60s alpha=0.5 drho=0.01dt No.=198,199,200
No.=200
No.=199
No.=198
level
w
40
30
20
10
0
−1
0
1
2
3
4
5

Figure 15:

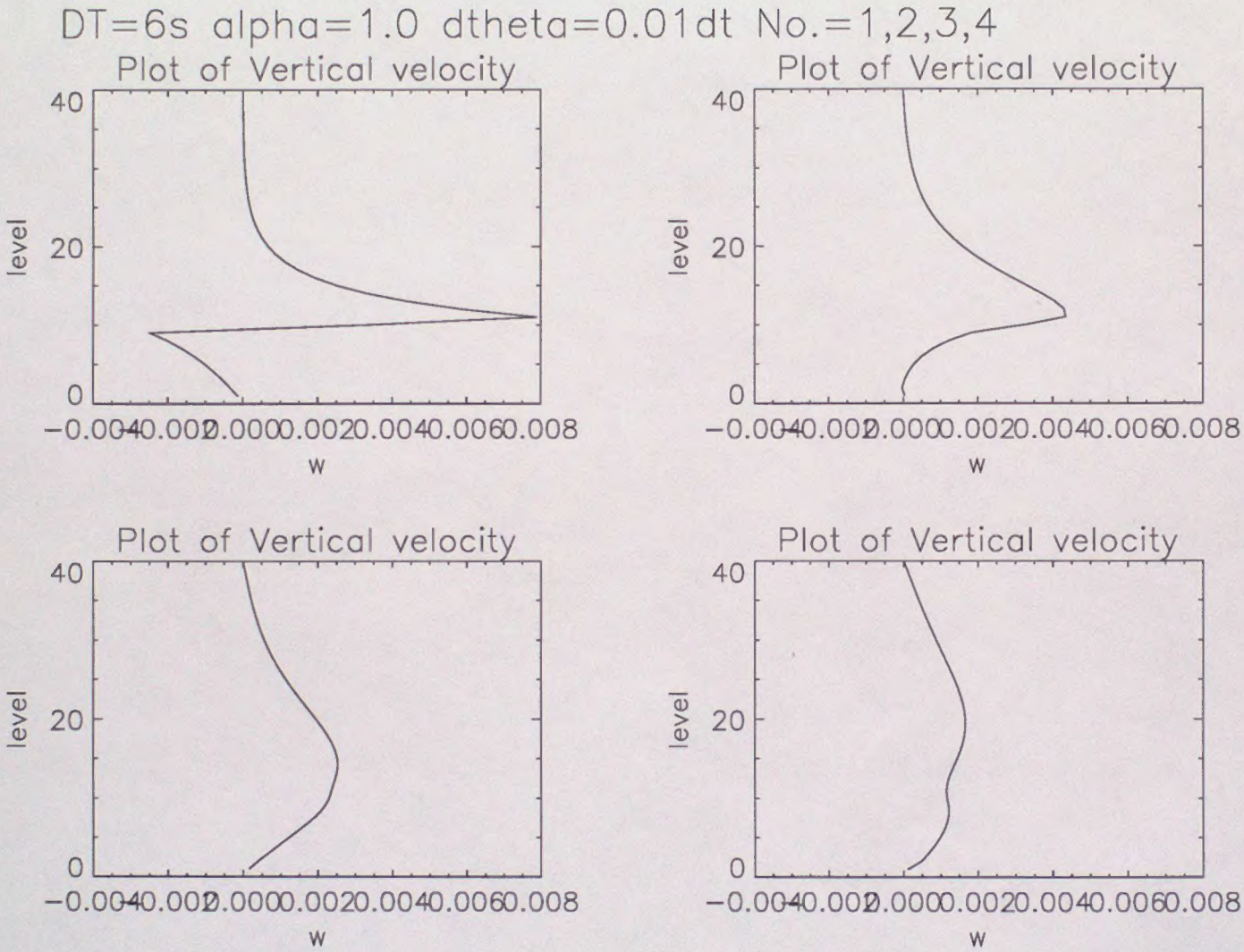
DT=6s alpha=1.0 dtheta=0.01dt No.=1,2,3,4
Plot of Vertical velocity
level
40
20
0
−0.004 −0.002 0.000 0.002 0.004 0.006 0.008
w
Plot of Vertical velocity
level
40
20
0
−0.004 −0.002 0.000 0.002 0.004 0.006 0.008
w
Plot of Vertical velocity
level
40
20
0
−0.004 −0.002 0.000 0.002 0.004 0.006 0.008
w
Plot of Vertical velocity
level
40
20
0
−0.004 −0.002 0.000 0.002 0.004 0.006 0.008
w

Figure 16:

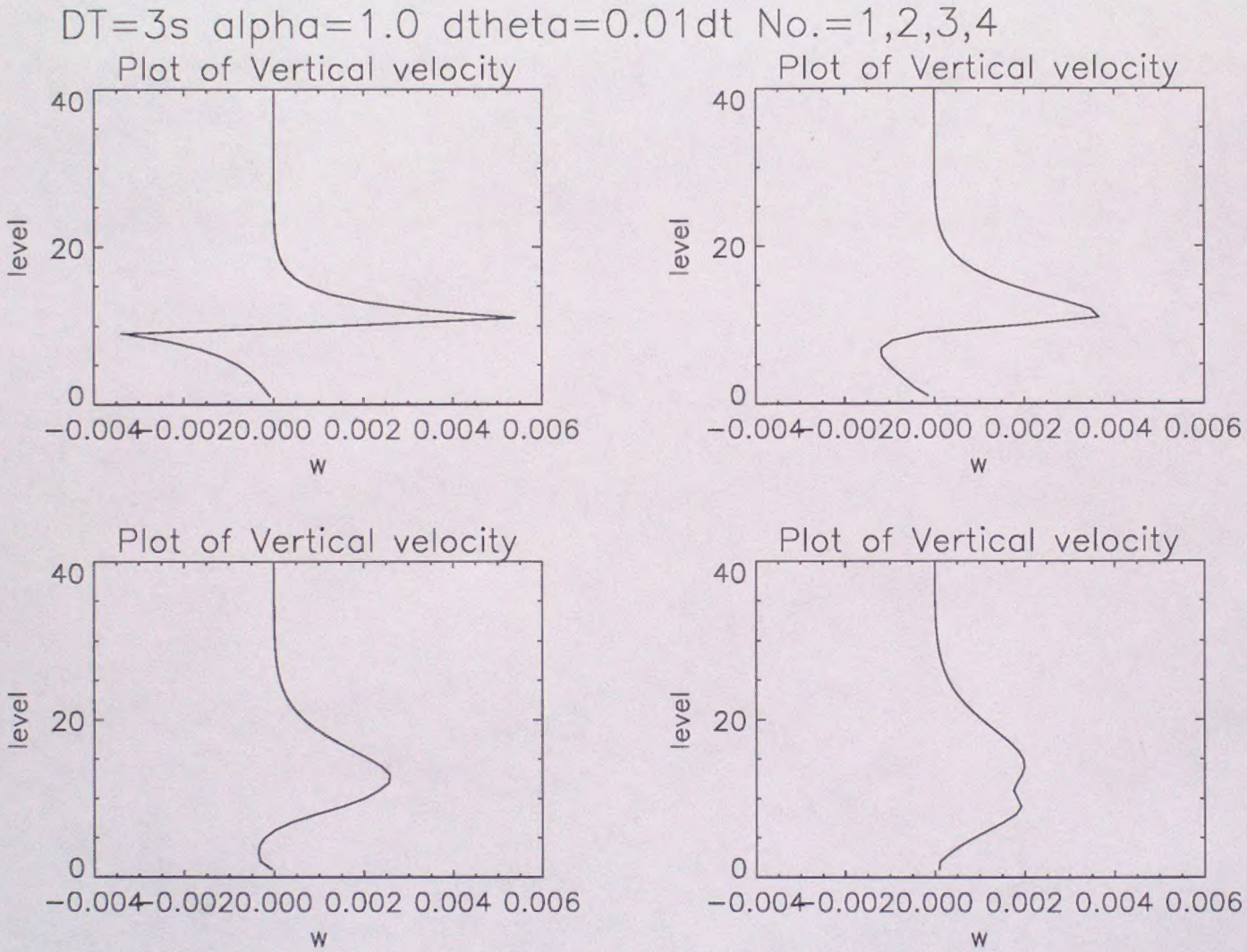
DT=3s alpha=1.0 dtheta=0.01dt No.=1,2,3,4
Plot of Vertical velocity
level
40
20
0
−0.004−0.0020.000 0.002 0.004 0.006
w
Plot of Vertical velocity
level
40
20
0
−0.004−0.0020.000 0.002 0.004 0.006
w
Plot of Vertical velocity
level
40
20
0
−0.004−0.0020.000 0.002 0.004 0.006
w
Plot of Vertical velocity
level
40
20
0
−0.004−0.0020.000 0.002 0.004 0.006
w

Figure 17: